NANO LETTERS

2008
Vol. 8, No. 9
2788-2793

Reassessing Fast Water Transport Through Carbon Nanotubes

John A. Thomas and Alan J. H. McGaughey*

Department of Mechanical Engineering, Carnegie Mellon University, Pittsburgh, Pennsylvania 15213

Received May 12, 2008; Revised Manuscript Received June 25, 2008

ABSTRACT

Pressure-driven water flow through carbon nanotubes (CNTs) with diameters ranging from 1.66 to 4.99 nm is examined using molecular dynamics simulation. The flow rate enhancement, defined as the ratio of the observed flow rate to that predicted from the no-slip Hagen-Poiseuille relation, is calculated for each CNT. The enhancement decreases with increasing CNT diameter and ranges from 433 to 47. By calculating the variation of water viscosity and slip length as a function of CNT diameter, it is found that the results can be fully explained in the context of continuum fluid mechanics. The enhancements are lower than previously reported experimental results, which range from 560 to 100 000, suggesting a miscalculation of the available flow area and/or the presence of an uncontrolled external driving force (such as an electric field) in the experiments.

Introduction. The flow rates of pressure-driven water through membranes of 1.6 and 7 nm diameter carbon nanotubes (CNTs), as measured by Holt et al.[1] and Majumder et al.,[2] are two to five orders-of-magnitude greater than those predicted by the continuum-based no-slip Hagen-Poiseuille relation. These findings have generated excitement in the molecular sieving, chemical detection, and drug delivery fields, where such high flow rates would significantly increase device efficiency, accuracy, and throughput.[3]

The nonwetting nature of CNTs suggests that the flow rate enhancement is caused by liquid slip at the water/carbon boundary. Using the slip-modified Hagen-Poiseuille relation with a bulk water viscosity, Holt et al. predict that slip lengths up to 1.4 μm would be necessary to reproduce their measured flow rates.[1] The required slip lengths for the 7 nm CNTs studied by Majumder et al. range from 39 μm to 54 μm.[2] For water flow in a single 250 nm diameter CNT, this range of slip lengths would enhance flow by a factor of 10 to 50 over the no-slip Hagen-Poiseuille relation. Sinha et al., however, who measured water flow through such a CNT, detected no order-of-magnitude flow enhancement.[4] Moreover, predictions from molecular dynamics (MD) simulations indicate that the water/graphene slip length is between 14 and 63 nm.[5]

Recognizing that the 1.4 μm to 54 μm slip lengths calculated by Holt et al. and Majumder et al. are 100 to 1000 times larger than typical slip lengths at nonwetting liquid/solid boundaries,[5] some have challenged the applicability of the Hagen-Poiseuille relation to the flow of water in sub-10 nm CNTs.[6] Others[3] have suggested that the enhanced flow is related to the subcontinuum, single-file molecular transport phenomenon identified in a 0.8 nm diameter CNT by Hummer et al. using MD simulation.[7] While computational/theoretical efforts have been made to predict the velocity profile inside CNTs[8] and determine the mechanisms responsible for slip at the water/CNT boundary,[9] a systematic investigation into the relationship between pressure gradient, flow rate, and tube diameter has not yet been performed.

In this investigation, we use MD simulation to investigate pressure-driven water flow through seven armchair CNTs with diameters between 1.66 and 4.99 nm. We begin by using nonequilibrium simulation to (i) identify the relationship between pressure gradient and volumetric flow rate and (ii) measure the radial velocity profile. Next, we use equilibrium simulation to predict the viscosity of water inside in each tube. Finally, from the calculated viscosity, pressure gradient, and velocity profile, we predict the slip length inside each CNT. We use this data to demonstrate that, even in CNTs with diameters as small as 1.66 nm, water flow is accurately described by the slip-modified Hagen-Poiseuille relation. Although our measured flow rates exceed those predicted from the no-slip Hagen-Poiseuille relation, we find no evidence for the enhancement reported by Majumder et al. or the upper range of enhancements reported by Holt et al. We hypothesize that the experimental findings are a result of a miscalculation of the available flow area or the presence of an uncontrolled experimental variable (e.g., an electric field).

Background. When subject to a pressure gradient, $\partial P/\partial z$, the radial velocity profile, $u(r)$, of an incompressible laminar liquid flowing steadily through a tube of radius R is

* Corresponding author.

10.1021/nl8013617 CCC: $40.75
Published on Web 07/30/2008

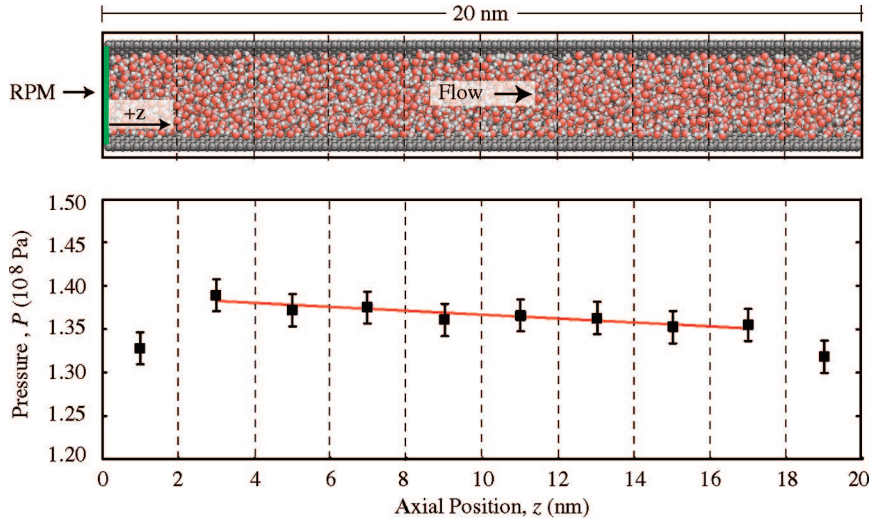

Figure 1. Axial pressure gradient inside the 2.77 nm diameter CNT. The pressure within each subvolume is predicted using the virial expansion method described by Allen and Tildesley.[16] Within the sampling region, the variation in liquid density with axial position is less than 1%.

$$u(r) = \frac{R^2}{4\mu}\left[1 - \frac{r^2}{R^2} + \frac{2L_s}{R}\right]\frac{\partial P}{\partial z} \tag{1}$$

where μ is the viscosity of the fluid and L_s is the slip length at the liquid/solid boundary. The slip length, which describes the velocity discontinuity between the liquid and the solid, is defined as [10−12]

$$L_s = \left.\frac{u(r)}{du/dr}\right|_{r=R} \tag{2}$$

The volumetric flow rate with slip, Q_S, is then given by

$$Q_S = \frac{\pi[(d/2)^4 + 4(d/2)^3 Ls]}{8\mu}\frac{\partial P}{\partial z} \tag{3}$$

where d (= $2R$) is the tube diameter. Equation 3 is the slip-modified Hagen-Poiseuille relation; the no-slip Hagen-Poiseuille flow rate, Q_N, is found by setting L_s equal to zero.

The flow rate enhancement, ε, reported by Holt et al. and Majumder et al. is defined as the ratio of the measured flow rate to Q_N (evaluated using a bulk viscosity and the CNT diameter). If the measured flow is modeled using eq 3, the enhancement becomes

$$\varepsilon \equiv \frac{Q_S}{Q_N} = \left[1 + 8\frac{L_s(d)}{d}\right]\frac{\mu_\infty}{\mu(d)} \tag{4}$$

where μ_∞ is the viscosity of bulk water, $L_s(d)$ is the diameter-dependent slip length, and $\mu(d)$ is the diameter-dependent viscosity of the water inside the CNT. When $\mu(d)$ is equal to μ_∞, the effects of slip on ε are only significant when $L_s(d) \geq d$. When $L_s(d) \ll d$ and $\mu(d) = \mu_\infty$, there will be no detectable enhancement relative to predictions from the no-slip Hagen-Poiseuille relation.

Data Collection. We use MD simulation to examine pressure-driven water flow through 1.66, 2.22, 2.77, 3.33, 3.88, 4.44, and 4.99 nm diameter single-walled armchair CNTs. A snapshot of a typical water/CNT system is presented in Figure 1, and the chirality vector for each CNT is listed in Figure 2. Interactions between water molecules are modeled using the TIP5P potential,[13] and interactions between water molecules and carbon atoms are modeled using the Lennard-Jones potential of Werder et al.[14] Simulations are performed in the *NVT* ensemble (constant number of particles, volume, and temperature) at a temperature of 298 K.

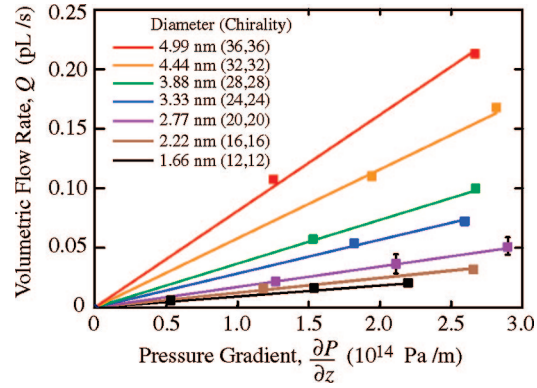

Figure 2. Volumetric flow rate in the CNTs versus pressure gradient. Over the pressure range investigated here, Q is directly proportional to $\partial P/\partial z$. Error bars, as shown for the 2.77 nm diameter CNT, are similar for all points, and the chirality vector for each CNT is listed in the legend.

For computational efficiency, we simulate water flow through single-walled CNTs with fixed carbon atoms.[12,18] Although stable single-walled nanotubes with diameters greater than 1.5 nm are difficult to fabricate, we have found that molecular behavior near multiwalled nanotubes is indistinguishable from that near single-walled CNTs due to the short-range of the carbon−water interaction. Thus, the results from our single-walled nanotube simulations can be applied to multiwalled nanotubes with similar interior or exterior diameters.

To predict the equilibrium water density inside the CNTs, we simulated an open-ended sample of each nanotube in a large water bath at a temperature and pressure of 298 K and 1 atm.[15] The bath density away from the tube was maintained at 1000 kg/m^3, and water molecules were able to freely diffuse across the open ends of the tube. After 250 ps, the

number of molecules enclosed inside the tube became steady in time, allowing us to determine the equilibrium density. The CNTs used in this study were filled with the number of molecules corresponding to this equilibrium density. Each CNT contains between 3100 and 6769 water molecules, corresponding to tube lengths that vary from 80 nm (for the 1.66 nm diameter CNT) to 12 nm (for the 4.99 nm diameter CNT). The water density inside each CNT is consistent with the densities reported by others.[8,18]

A pressure gradient and flow field are established inside the tube by placing a reflecting particle membrane (RPM)[17] at $z = 0$ (periodic boundary conditions are imposed in the z-direction). The RPM operates as follows: molecules crossing the membrane in the desired flow direction pass freely; molecules crossing the membrane in the opposite direction have some probability, p, of being elastically reflected in the flow direction. The water flow rate and magnitude of the pressure gradient inside the tube are tuned via the magnitude of p. As depicted in Figure 1, we calculate $\partial P/\partial z$ by evaluating the pressure within several subvolumes along the tube axis and performing a linear regression analysis. Since we know the position and momentum of each particle in the simulation, the radial velocity profile can be calculated directly. The volumetric flow rate is then found by integrating the velocity profile over the CNT cross-sectional area. Since water molecules remain at least 0.2 nm away from the CNT surface[8,15,18] (i.e., there is no flow in these regions), we note that the actual flow diameter is smaller than the full CNT diameter d that we, remaining consistent with Holt et al. and Majumder et al., use to calculate Q_N and ε.

In Figure 2, we present the volumetric flow rate versus pressure gradient for all seven CNTs. Each data point is the average of at least 5 independent trials, which consist of a 250 ps equilibration period (during which the flow system reaches a steady state) followed by a 300 ps data collection period. The mean flow velocities are 3−14 m/s. Because of the time scales accessible in MD (a few nanoseconds), we cannot resolve the experimental mean flow velocities of 0.01−1 m/s. However, the linear relationship between the flow rate and the pressure gradient, which is consistent with eq 3, suggests that our results will be applicable to the flow rates realized in the experiments. Unlike previous MD simulations of water flow through CNTs, where the mean flow velocities were 100−300 m/s,[8,18] we are well-below the molecular thermal velocity (340 m/s at a temperature of 298 K).

In Figure 3, we present the flow enhancement versus CNT diameter for the seven CNTs. For comparison purposes, we also plot the enhancement corresponding to a bulk viscosity ($\mu_\infty = 0.89$ mPa·s; see below) and our predicted slip length for water flow past a flat graphene sheet ($L_{s,\infty} = 30$ nm; see below). These results have three important features. First, the magnitude of the flow enhancement decreases with increasing CNT diameter. Second, with increasing diameter, our predicted enhancement converges to that predicted from eq 4 with a 30 nm slip length and a bulk viscosity. This finding is opposite to the results of Majumder et al. compared

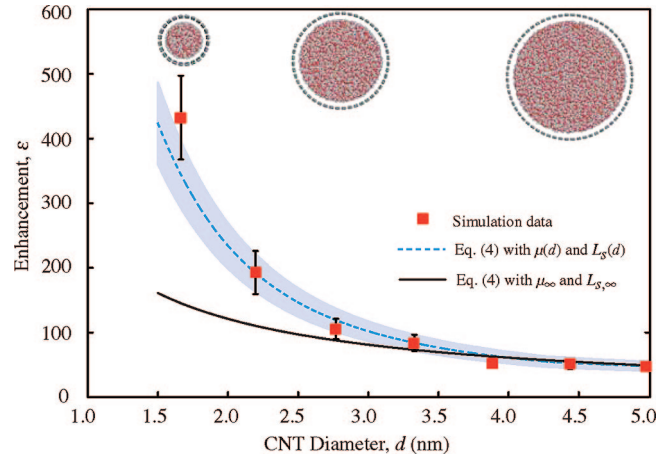

Figure 3. Flow enhancement (calculated flow rate divided by Q_N) as predicted from MD simulations. Superimposed on the simulation data is the enhancement predicted from eq 4 with $L_s = 30$ nm and $\mu(d) = \mu_\infty$, and the enhancement predicted from eq 4 using a CNT-specific slip length and viscosity. The shading indicates our 15% uncertainty in the predicted viscosity and slip length data, and the error bars indicate our 15% uncertainty in the calculated flow rates. The enhancement range reported by Holt et al. for 1.6 nm CNTs is $560 < \varepsilon < 9600$. A point corresponding to the flow enhancement through 7 nm diameter CNTs reported by Majumder et al. would have an ε value of 50 000, approximately 100 times greater than the maximum value on our plot.

with those of Holt et al., which suggest that the flow enhancement (relative to the no-slip predictions) increases by a factor of 10−100 as the mean CNT diameter is increased from 1.6 to 7 nm. Third, the variation in ε with CNT diameter cannot be captured using a single slip length. This result is consistent with previous simulations of simple fluids confined inside CNTs, where both the slip length and the viscosity were found to be dependent on CNT diameter.[12] A CNT-specific water viscosity and slip length (not bulk water properties and a uniform slip length) should therefore be used when making comparisons between the MD-measured enhancement and that predicted from eq 4.

Viscosity and Slip Length Predictions. In Figure 4, we present the water viscosity versus CNT diameter for all seven CNTs. We predict the viscosity from the axial self-diffusion coefficient, D_z, by evoking the Einstein relation[19−21]

$$\mu = \frac{k_B T}{3\pi a} \frac{1}{D_z} \tag{5}$$

where k_B is the Boltzmann constant and a is the molecular diameter (taken to be 0.17 nm from the average positions of the hydrogen atoms and charge sites relative to the oxygen atom in the TIP5P water model [13]). We predict D_z from the Green-Kubo linear response relation[16]

$$D_z = \frac{1}{N} \sum_{i=0}^{N} \int_0^\infty \langle v_{i,z}(t) \cdot v_{i,z}(0) \rangle \, dt \tag{6}$$

where t is time and $v_{i,z}$ is the axial center-of-mass velocity of molecule i. The brackets denote an autocorrelation and the summation is over all molecules, N. Unlike in smaller diameter CNTs, where multiple regimes of diffusion have been reported,[26] D_z for each of our tubes is invariant with autocorrelation length.

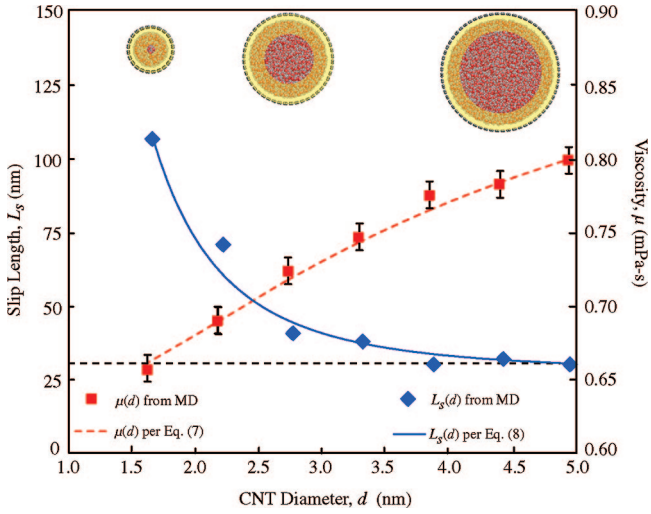

Figure 4. Variation of viscosity and slip length with CNT diameter. The MD viscosity was predicted from equilibrium simulation using eq 5. The highlighted annular regions on the CNT snapshots indicate the interface area used to evaluate eq 7. The MD slip length was evaluated from the velocity profile inside each CNT and eq 2. The variation in slip length with CNT diameter is fit using eq 8 with $C = 352$ nm^4. The dashed horizontal line identifies $L_{s,\infty}$ (=30 nm). The uncertainty in the slip length is ±1 nm, making the error bars smaller than the data points.

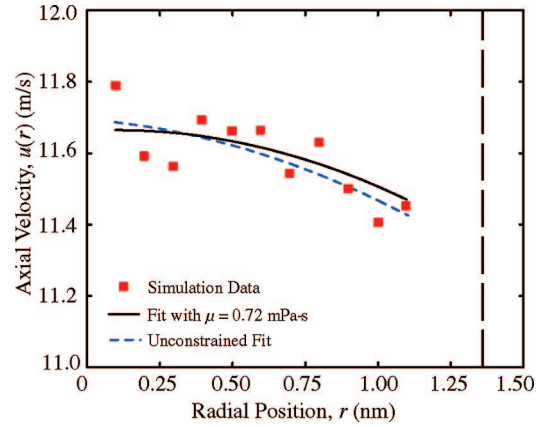

Figure 5. Radial velocity profile inside 2.77 nm diameter CNT fit using both unconstrained and constrained fitting procedure. The vertical dashed line at 1.38 nm represents the CNT surface. As discussed in the text, water molecules remain 0.2 nm from the CNT surface. The standard deviation for each point is approximately 2 m/s. On the basis of a χ^2 goodness-of-fit test,[31] we can state with a 90% confidence interval that the data used to generate this profile is consistent with our parabolic constrained fit. This confidence interval increases to 95% for the 2.22 nm CNT and to 99% for all of the larger tubes.

To test the validity of eq 5, we performed equilibrium simulations of bulk water at a temperature of 298 K and pressure of 1 atm. Our calculated self-diffusion coefficient is 2.63×10^{-9} m^2/s, which matches the TIP5P self-diffusion coefficient reported by Mahoney and Jorgensen.[22] In using this self-diffusion coefficient and the molecular diameter of 0.17 nm, the viscosity calculated from eq 5 is 1.02 mPa•s. This value is in good agreement with the experimentally measured value of 0.89 mPa•s[23] and the 1.06 mPa•s value we predict directly from MD simulations and Green-Kubo linear response theory.[16]

Since both the diffusion coefficient[25] and the viscosity[24] of liquids near solid surfaces are spatially varying, we recognize that our calculated viscosity represents a cross-sectional averaged effective viscosity. We find that our viscosities are well-described by a weighted-average of the viscosities in the interface and bulk-like regions in the CNT cross section,

$$\mu(d) = \mu_i \frac{A_i(d)}{A_t(d)} + \mu_\infty \left[1 - \frac{A_i(d)}{A_t(d)}\right] \tag{7}$$

where μ_i and A_i are the viscosity and area of the interface region, and A_t is the total cross-sectional area. On the basis of previous investigations,[15,25] we define the interface to be the annular region located within 0.7 nm of the CNT surface, as illustrated in Figure 4. We set μ_i equal to the viscosity inside the 1.66 nm diameter CNT (where the interface region covers 97% of the cross-sectional area). In CNTs with diameters smaller than 1.66 nm, where the tube diameter is less than 10 times the water molecule diameter and subcontinuum transport phenomena are present, eq 7 will not accurately predict the water viscosity.[26,27]

We predict the slip length of the confined water from the radial velocity profiles measured during the nonequilibrium flow simulations. By fitting each velocity profile to the parabolic function $u(r) = Ar^2 + B$, we can directly calculate L_s from eq 2. We constrain the fit such that A and B satisfy the viscosity predicted inside each CNT from our equilibrium simulation. This approach is in contrast to that of Sokhan et al.,[12] who fit both the viscosity and the slip length to the velocity profile.

To illustrate this procedure, consider the velocity profile for the 2.88 nm CNT presented in Figure 5. If we use the procedure of Sokhan et al., the viscosity is 0.42 mPa•s and the slip length is 24 nm. Since this viscosity is below the value of 0.72 mPa•s predicted from our equilibrium simulation, the calculated slip length will be underestimated. If we constrain the fit, the viscosity is set to 0.72 mPa•s and slip length becomes 41 nm. The slip lengths for all seven CNTs, as calculated using constrained fits, are presented in Figure 4. We suspect that the unconstrained fit procedure may be responsible for the anomalously small slip lengths reported by Sokhan et al.[12]

Petravic and Harrowell[32] have developed a linear response procedure for calculating the slip length at planar liquid/solid boundaries. While this approach cannot be applied to cylindrical systems where there is only one solid surface, it can be used to validate our slip length calculation procedure. We begin by performing equilibrium simulations of water between two infinite graphene sheets separated by 5 nm. Using the procedure of Petravic and Harrowell, we predict a water/graphene slip length of 30 nm. Next, we induce water flow through the channel and evaluate the velocity profile. Using the velocity fitting procedure discussed above, we calculate a slip length of 31 nm. The predicted slip lengths are within the ±1 nm uncertainty we associate with both techniques. We also note that, using the 10 nm hydraulic diameter of the channel, the viscosity predicted from the weighted-average relation presented in eq 7 is 0.88 mPa•s.

This value agrees with the value of 0.83 mPa•s we predict using the Einstein relation presented in eq 5.

Liquid slip at the solid/liquid boundary is a rate process limited by the ability of molecules to hop between open surface lattice sites.[28] The slip length is therefore large when the solid/liquid binding energy is weak and the solid/liquid potential energy landscape near the solid surface is smooth. In a previous report, we demonstrated and discussed how decreasing the CNT diameter weakens the coupling between water molecules and the carbon surface.[15] We attribute the increase in slip length with decreasing CNT diameter to this phenomenon. We also showed previously how the effect of surface curvature on the potential energy landscape becomes negligible as the CNT diameter is increased beyond 5 nm.[15] This trend explains why the slip length converges to 30 nm, the slip length we predict for a flat graphene sheet, as the CNT diameter increases. As shown in Figure 4, this variation in slip length with CNT diameter is well-described by the empirical relation

$$L_s(d) = L_{s,\infty} + \frac{C}{d^3} \tag{8}$$

where $L_{s,\infty}$ (= 30 nm) is the slip length over a flat graphene sheet and C is a fitting parameter.

Kassinos et al. previously reported water/CNT slip lengths of 10, 12, and 18 nm in 2.71, 4.07, and 5.42 nm diameter CNTs.[29] These values, however, as calculated represent the "excess radius", R_x, and not the water/CNT slip length, L_s. The excess radius is the difference between the radial position at which the velocity profile would become zero and the radial position of the solid surface, and is only equivalent to the slip length when the velocity profile is linear.

Comparisons and Discussion. In Figure 3, we compare the flow enhancement, as measured from our nonequilibrium simulations, to that calculated using eq 4 with the viscosity and slip length data presented in Figure 4. For the CNTs with diameters between 2.11 to 4.99 nm, the enhancement predicted from eq 4 is within 10% of the enhancement measured during the simulation. For the 1.66 CNT, the values are within 25%. This excellent agreement, coupled with the parabolic velocity profiles detected in the CNTs, indicate that flow through CNTs with diameters greater than and equal to 1.66 nm can be modeled using the slip-modified Hagen-Poiseuille formulation. This finding is consistent with previous investigations of simple fluids, where flow could be modeled using tools from continuum theory when the characteristic flow dimension is at least 10 times the molecular diameter.[17,30]

In the 1.66 nm CNT, our predicted flow enhancement is 433. This value is comparable to the lower end of the 560 to 9600 enhancement range measured by Holt et al. Our predicted flow enhancement inside the 2.22 nm CNT is 184, which is comparable to the enhancement of 459 we calculate from the data of Joseph and Aluru for a tube of similar diameter.[18] Although Joseph and Aluru report an enhancement factor of 2052, they calculated Q_N using a CNT diameter inconsistent with that of Holt et al. and Majumder et al. The diameter used by Holt et al. and Majumder et al. when calculating Q_N is the CNT diameter; the diameter used by Joseph and Aluru was found by subtracting twice the Lennard-Jones length scale [σ (= 0.339 nm)] for carbon atoms from the CNT diameter. Using the full CNT diameter reduces their predicted enhancement from 2052 to 459.

The flow enhancements through 7 nm diameter CNTs, as reported by Majumder et al., are 10 000 to 100 000. Although computational limitations prevent us from simulating water flow through such large tubes, our data does not support their experimental results. By using eq 7, the effective viscosity inside a 7 nm diameter tube will be 0.85 mPa•s. The effects of surface curvature are nearly negligible in a 7 nm diameter CNT, and the slip length will be close to the 30 nm flat-sheet limit. Such conditions should increase flow by a factor of only 35. In larger 250 nm CNTs, our models suggests that water flow would exceed predictions from the no-slip Hagen-Poiseuille relation by a factor of only 2. This result may explain why Sinha et al.[4] detected no flow enhancement.

To improve the MD predictions, a more sophisticated interatomic potential that includes the effects of polarization[33] (but increases the computational demands by more than 1 order of magnitude) could be used. We could also allow the carbon atoms to move (which could change the flow rate by 10 to 20%[12,18]) and consider multiwalled CNTs (as used in experiments). While these enhancements might bring our predictions into better agreement with the lower-end of the enhancement range reported by Holt et al., it does not seem possible that they could explain the results of Majumder et al. While we recognize that calculating flow areas and measuring water flow rates through CNT membranes is a challenging process, the very large experimental enhancements are difficult to justify. The results of Holt et al. and Majumder et al. suggest to us a miscalculation of the available flow area and/or the presence of an uncontrolled external driving force (such as an electric field[34]) in their experiments.

Acknowledgment. This work was supported by an NSF Graduate Research Fellowship (J.A.T.) and the Berkman Faculty Development Fund.

References

(1) Holt, J. K.; Park, H. G.; Wang, Y.; Stadermann, M.; Artyukhin, A. B.; Grigoropoulos, C. P.; Noy, A.; Bakajin, O. *Science* **2006**, *312*, 1034–1037.
(2) Majumder, M.; Chopra, N.; Andrews, R.; Hinds, B. J. *Nature* **2005**, *438*, 44.
(3) Noy, A.; Park, H. G.; Fornasiero, F.; Holt, J. K.; Grigoropoulos, C. P.; Bakajin, O. *Nanotoday* **2001**, *2*, 22–29.
(4) Sinha, S.; Rossi, M. P.; Mattia, D.; Gogotsi, Y.; Bau, H. H. *Physics of Fluids* **2007**, *19*, 013603.
(5) Koumoutsakos, P.; Jaffe, R. L.; Werder, T.; Walther, J. H. *Nanotech.* **2003**, *1*, 148–151.
(6) Verweij, H.; Schillo, M. C.; Li, J. *Small* **2007**, *3*, 1996–2004.
(7) Hummer, G.; Rasaiah, J. C.; Noworyta, J. P. *Nature* **2001**, *414*, 188–190.
(8) Hanasaki, I.; Nakatani, A. *J. Chem. Phys.* **2006**, *124*, 144708.
(9) Joseph, P.; Cottin-Bizonne, C.; Benoit, J.-M.; Ybert, C.; Journet, C.; Tabeling, P.; Bocquet, L. *Phys. Rev. Lett.* **2006**, *97*, 156104.
(10) Joseph, P.; Tabeling, P. *Phys. Rev. E* **2005**, *71*, 035303.
(11) Barrat, J.-L.; Chiaruttini, F. *Mol. Phys.* **2003**, *101*, 1605–1610.
(12) Sokhan, V. P.; Nicholson, D.; Quirke, N. *J. Chem. Phys.* **2002**, *117*, 8531–8539.
(13) Mahoney, M. W.; Jorgensen, W. L. *J. Chem. Phys.* **2000**, *112*, 8910–8922.

(14) Werder, T.; Walther, J. H.; Jaffe, R. L.; Halicioglu, T.; Koumoutsakos, P. *J. Phys. Chem. B* **2003**, *107*, 1345–1352.
(15) Thomas, J. A.; McGaughey, A. J. H. *J. Chem. Phys.* **2008**, *128*, 084715.
(16) Allen, M. P. and Tildesley, D. J. *Computer Simulation of Liquids*; Clarendon Press: Oxford, 1987.
(17) Li, J.; Liao, D.; Yip, S. *Phys. Rev. E* **1998**, *57*, 7259–7267.
(18) Joseph, S.; Aluru, N. R. *Nano Lett.* **2008**, *8*, 452–458.
(19) McQuarrie, D. A. *Statistical Mechanics*; Viva Books Private Limited: New Delhi, 2005.
(20) Heyes, D. M. *The Liquid State: Applications of Molecular Simulations*; Wiley and Sons: New York, 1998.
(21) Yongli, S.; Minhua, S.; Weidong, C.; Congxiao, M.; Fang, L. *Comput. Mater. Sci.* **2007**, *38*, 737–740.
(22) Mahoney, M. W.; Jorgensen, W. L. *J. Chem. Phys.* **2001**, *114*, 363–366.
(23) Cengel, Y. A. and Cimbala, J. M. *Fluid Mechanics: Fundamentals and Applications*; McGraw-Hill Higher Education: New York, 2006.
(24) Pozhar, L. A. *Phys. Rev. E* **2000**, *61*, 1432–1446.
(25) Thomas, J. A.; McGaughey, A. J. H. *J. Chem. Phys.* **2007**, *126*, 034707.
(26) Striolo, A. *Nano Lett.* **2006**, *6*, 633–639.
(27) Hansen, J. S.; Daivis, P. J.; Travis, K. P.; Todd, B. D. *Phys. Rev. E* **2007**, *76*, 041121.
(28) Lichter, S.; Martini, A.; Snurr, R. Q.; Wang, Q. *Phys. Rev. Lett.* **2007**, *98*, 226001.
(29) Kassinos, S. C.; Walther, J. H.; Kotsalis, E. M. ; Koumoutsakos, P. In *Multiscale Modelling and Simulation*; Attinger, S., Koumoutsakos, P., Eds.; Springer: New York, 2004; pp 220−224..
(30) Travis, K. P.; Todd, B. D.; Evans, D. J. *Phys. Rev. E* **1997**, *55*, 4288–4295.
(31) Kenkel, J. L. Duxbury Press: Belmont, California, 1996.
(32) Petravic, J.; Harrowell, P. *J. Chem. Phys.* **2007**, *127*, 174706.
(33) DeFusco, A.; Schofield, D. P.; Jordan, K. D. *Mol. Phys.* **2007**, *105*, 2681–2696.
(34) Wang, Z.; Ci, L.; Nayak, S.; Ajayan, P. M.; Koratkar, N. *Nano Lett.* **2007**, *7*, 679–702.

NL8013617